Catalysis Today 299 (2018) 112–119

Contents lists available at ScienceDirect

Catalysis Today

journal homepage: www.elsevier.com/locate/cattod

# Low temperature methanol synthesis catalyzed by copper nanoparticles

Christian Ahoba-Sam[a], Unni Olsbye[b], Klaus-Joachim Jens[a,*]

[a] Department of Process, Energy and Environmental Technology, University College of Southeast Norway, Kjølnes Ring 56, 3918 Porsgrunn, Norway
[b] Department of Chemistry, University of Oslo, P.O. Box 1033, Blindern, N-0315 Oslo, Norway

ARTICLE INFO

*Keywords:*
Methanol synthesis
Low temperature
Cu
Nanoparticle size
Deactivation

ABSTRACT

A one pot catalytic system which involves Cu and an alkoxide co-catalyst has been used for methanol (MeOH) synthesis at low temperature. Up to about 92% syngas conversion per pass and more than 90% selectivity to MeOH (the rest is methyl formate) was obtained depending on the amount of catalyst employed at 100 °C and 20 bar syngas pressure. Low temperature methanol synthesis presents a good alternative to current technology for methanol production since the former is thermodynamically favored and gives a high yield per pass. Cu particles sized around 10 ± 5 nm were found to be involved in the catalytic process. Cu nanoparticles of increasing size was synthesized by varying temperature. However, methanol production decreased with increasing Cu nanoparticle size. Moreover, the maximum conversion at the end of each successive batch declined as a function of the number of cycles performed. Decrease in catalyst activity corresponded to Cu nanoparticle densification, suggesting agglomeration to be a major catalyst deactivation pathway.

## 1. Introduction

Methanol (MeOH) has been identified as a potential multipurpose molecule for energy and $CO_2$ storage [1]. It stores both carbon and hydrogen in the liquid form, it is readily transportable and it serves as a base chemical for direct conversion into light olefins, gasoline and hydrocarbons over acidic zeolites [2], thereby providing an alternative to today's fossil energy sources and petrochemical feedstocks.

MeOH is currently synthesized from syngas (made up of $CO/CO_2/H_2$) over $Cu/ZnO/Al_2O_3$ catalysts, which operate at 250 °C and 70–100 bar of pressure [3,4]. Though this technology is highly optimized, it is capital intensive and syngas conversion per pass is thermodynamically limited. This is because conversion of syngas to methanol is an exothermic reaction (Eq. (1)) and lower temperature is required to achieve full conversion per pass. Furthermore, syngas production accounts for more than half of the total capital cost in current methanol processes [5]. Complete syngas conversion per pass will allow use of air instead of pure oxygen in the syngas section of the methanol process. This will significantly reduce the overall cost in methanol synthesis. Hence, there is a need for low temperature methanol synthesis catalysts.

$$CO + 2H_2 \leftrightarrow CH_3OH \quad \Delta H = -90.6 kJ/mol \tag{1}$$

A low temperature methanol synthesis (LTMS) reaction was identified by Christiansen in 1919 [6], which presented the possibility of almost full syngas conversion to MeOH per pass at low temperature (120 °C) conditions. This approach is known to involve firstly, carbonylation of methanol to form methyl formate (MF) and secondly, MF hydrogenolysis to form MeOH as indicated in Eqs. (2) and (3), leading to Eq. (1) as the overall reaction.

$$CO + CH_3OH \leftrightarrow HCOOCH_3 \tag{2}$$

$$HCOOCH_3 + 2H_2 \leftrightarrow 2CH_3OH \tag{3}$$

It is suggested that alkali metal promotes alcohol (methanol) carbonylation by forming metal alkoxide which has an increased electron density on their oxygen compared to the oxygen on alcohols [7]. The hydrogenolysis of the MF is suggested to occur via a formaldehyde intermediate [8] and subsequent reduction to form MeOH.

Catalyst systems reported in previous works for the carbonylation and hydrogenolysis steps of the LTMS reaction are a combination of an alkali-metal, an alcohol solvent and a transition-metal compound. Various Ni-based compounds such as $Ni(CO)_4$ and $Ni(OCOCH_3)_2$ in combination with alkali-metal alkoxide co-catalysts have been shown to be very active for syngas conversion between 80 to 120 °C and 10 to 50 bar [9,10]. However, the metal alkoxide component of the catalyst forms a stable hydroxide when in contact with water, and therefore brings the reaction to a halt. Furthermore, the tetracarbonyl nickel [10] complex is volatile and highly toxic [11], and therefore poses a potential handling risk on an industrial scale.

Copper-based materials have also been reported to be active methanol synthesis catalysts at 80–120 °C and 10–20 bar pressure. Raney

* Corresponding author.
*E-mail addresses:* christian.ahoba-sam@hit.no (C. Ahoba-Sam), unni.olsbye@kjemi.uio.no (U. Olsbye), Klaus.J.Jens@hit.no (K.-J. Jens).

http://dx.doi.org/10.1016/j.cattod.2017.06.038
Received 31 October 2016; Received in revised form 2 June 2017; Accepted 29 June 2017
Available online 01 July 2017

copper, copper on silica support, copper chromate as well as copper alkoxide are among the identified copper-based materials, though these are not as efficient as Ni [12–14]. The copper chromate catalyst seems to be most widely used. An enhanced catalytic activity is observed when physical mixture of $CuO/Cr_2O_3$ catalyst is milled by creating lattice defects leading to an increased surface area. [14,15].

We have focused on the copper alkoxide LTMS system. We could show that Raney copper works well as a LTMS hydrogenolysis catalyst [13]. Subsequently we reported the catalytic behavior of a $Cu(OCH_3)_2$/$NaH/CH_3OH$ catalyst system. This catalyst system exhibited 75% syngas conversion at 120 °C and 20 bar, showing however linear catalyst deactivation when syngas was charged multiple times [16]. In order to optimize this catalyst system, there is a need to characterize it and gain insight into the gradual catalyst activity decline.

In this work, we report Cu nanoparticles to be involved in the LTMS reaction. We present a simple method of making Cu nanoparticles which catalyze methanol synthesis at 100 °C and investigate the effect of Cu particle size on this reaction. Finally we characterized the catalyst after repeated test cycles.

## 2. Experimental section

### 2.1. Materials and experimental setup

Copper (II) acetate ($Cu[OAc]_2$, 98%), dry sodium hydride (NaH = 95%), methanol (MeOH, anhydrous 99.8%) and diglyme (1-methoxy-2-[2-methoxyethoxy]ethane, ≥99.5%) were purchased from Sigma Aldrich. The syngas made up of $1CO:2H_2$ ( ± 2%) was purchased from Yara Praxair AS. All chemicals were used as received unless otherwise stated.

The synthesis of both catalyst and methanol were done in a 200 ml (60 mm diameter) stainless steel high pressure type hpm-020 autoclave batch reactor (Premex Reactor AG). The reactor was equipped with a dip tube for sampling, pressure sensors and a thermocouple inserted into the reactor to monitor internal pressure and temperature respectively. A Nupro security valve was set at 100 bar for safety and the magnetic stirrer head was attached to a stirrer with oblique impeller blades (approximately 30 angle) which extended near to the bottom of the reactor to ensure adequate mixing. The magnetic stirrer head was externally attached to an electric BCH Servo Motor that is paired with lexium 23 drive to give between 1000 to 3000 rpm, with a high degree of precision. The reactor was heated in oil block controlled by a Huber Ministat 230 thermostat. The internal temperature and pressure in the reactor was independently logged onto a PC.

### 2.2. Copper catalyst preparation

Typically, about 3.6 mmol of $Cu(OAc)_2$, 18.5 mmol of dry NaH and 50 ml diglyme were placed in the reactor. Under $N_2$ blanket set to about 1 bar, the mixture was stirred at 3000 rpm and heated to a predetermined temperature for 2 h. The set point temperatures for Cu catalyst preparation were 80, 100, 126 or 149 °C for the different catalyst systems. Thereafter the reaction in the reactor was cooled to ambient temperature (< 30 °C) followed by 52 mmol MeOH addition. This mixture was stirred at ambient temperature for 30 min to ensure that all NaH had reacted to give the sodium methoxide co-catalyst. An approximate 2 ml sample was taken for analysis using the dip tube in-between the reaction steps.

### 2.3. Catalytic testing

The reactor with the remaining slurry described in Section 2.2 was purged with syngas and charged to about 20 bar, then stirred at 3000 rmp and heated to 100 °C. After 2 h the reactor was cooled to about 25 °C. Syngas conversion was determined by the difference in pressure between the start and after reactor cooling to room temperature. Typically, the amount of carbon products in liquid reaction mixture after cooling compared to the syngas pressure drop represented about 85 ± 2% of syngas consumed, assuming $CO/2H_2$ were proportionally consumed.

The liquid portion of the resulting reaction was sampled after it had been allowed to settle and was analyzed by gas chromatography equipped with both liquid and gas injection valves (Agilent 7890A). The liquid injection port was connected to a CARBOWAX 007 series 20 M column with dimensions 60 m × 320 µm × 1.2 µm; and was programmed as follows; temperature was ramped by 15 °C/min from 40 °C initial temperature to 200 °C and held at 200 °C for 3 min, at 0.47 bar (6.8 psi) constant pressure. The liquid sample was injected via an Agilent 7683 B autosampler. The products were identified and quantified by an Agilent 5975 mass spectrometer detector. 0.54 mg Heptane was used as internal standard and added to each sample vial. The gas injection valve was connected to 2.7 m Porapak Q and 1.8 m Molecular Sieve 5 Å packed columns connected to a TCD for analysis of permanent gases and up to $C_2$ hydrocarbons. This set-up was connected to a 0.9 m Hayesep Q back flush column.

### 2.4. Cu catalyst characterization

The Cu catalysts were analyzed by XRD and TEM before and after the low temperature methanol synthesis (LTMS) reaction. A Bruker D8 A25 powder diffractometer using Mo Kα radiation with wavelength, λ = 0.71076 Å and Lynxeye detector with “hardened” chip for Mo radiation was used. Total Pattern Analysis Solution (TOPAS) software was employed for quantitative Rietveld analysis of the diffractogram. This software operates by fitting theoretical diffraction pattern to a measured diffraction pattern using non-linear least square algorithms [17]. The samples were analyzed as slurry which was pipetted into a capillary tube with 0.5 mm internal diameter. The tube was centrifuged at 2000 rmp for 10 min to settle the solid portion at the bottom and was thereafter mounted on capillary spinner. X-ray diffractograms were measured at 0.023° step/s for an interval of 15–35° 2 θ.

The TEM imaging was performed with a Joel 2100F instrument. Samples were diluted in methanol, and particles were separated in an ultrasound bath for 30 min. The solution was then dropped on a carbon film on a copper grid. Cu particles were ascertained to be present using EDS and electron diffraction. Generally, particle sizes were determined by using the average of 15 particles diameter ± mean deviation from the TEM images for each sample.

Cu particles agglomeration effect on activity was estimated by assuming spherical Cu particles and constant total volume of Cu before and after deactivation.

$$\frac{Numberoffreshcuparticles}{NumberofspentCuparticles} = \left(\frac{VolumeoffreshCu}{VolumeofspentCu}\right)^{-1} \quad (4)$$

$$\frac{SurfaceareaoffreshCuparticles}{SurfaceareaofspentCuparticles} = \left(\frac{AreaoffreshCuparticles}{AreaofspentCuparticles}\right) \times \left(\frac{VolumeoffreshCu}{VolumeofspentCu}\right)^{-1} = \frac{DiameterofspentCuparticles}{DiameteroffreshCuparticles} \quad (5)$$

## 3. Results and discussion

### 3.1. Typical LTMS reaction at 100 °C

Fig. 1 shows the experimental procedure for a typical LTMS reaction. In step A, NaH is expected to react with $Cu^{2+}$ ions to give Cu in a reduced oxidation state, either $Cu^+$ or $Cu^0$ or a mixture of the two. In the former case CuH could be a possible reaction product as $Cu^+$ may react with $H^-$ although this compound is expected to be highly unstable at the working conditions [18]. Step A resulted in about 0.35 bar pressure increase, and was determined with GC/TCD to be $H_2$ (illustrated by Eq. (6)). Addition of excess MeOH in step B was to ensure

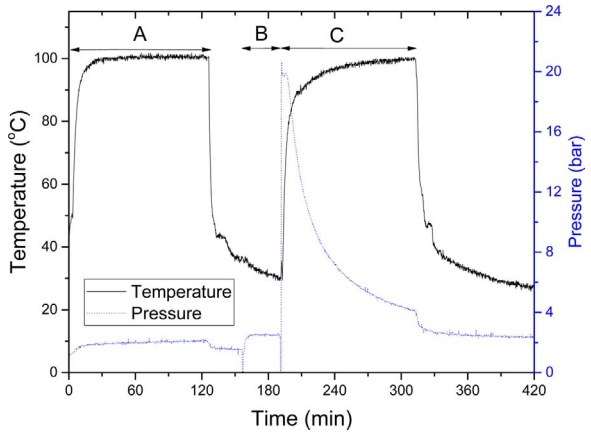


**Fig. 1.** Typical LTMS procedure employed in this work, A = 3.6 mmol Cu(OAc) 2 + 18 mmol NaH in 50 ml diglyme, B = addition of 49 mmol MeOH, C = 20 bar $2H_2$:1CO charged.

that all the NaH was consumed to produce $NaOCH_3$ which is the co-catalyst for the LTMS. After 30 mins of stirring, pressure increased by 1.38 bar as a result of $H_2$ evolution (according to Eq. (7)). Syngas was added at step C for the methanol synthesis at 100 °C. Syngas conversion was estimated based on pressure drop, and in this case, 89% syngas conversion was achieved.

$$Cu^{2+}_{(diglyme)} + 2H^{-} \rightarrow Cu + H_2 \quad (6)$$

$$NaH_{(s)} + CH_3OH_{(l)} \rightarrow CH_3ONa_{(diglyme)} + H_{2(g)} \quad (7)$$

To determine the oxidation state, composition and crystallite size of Cu in the slurry, XRD of the slurry was measured. Fig. 2a shows the X-ray diffractogram of the catalyst system after the steps A, B and C. Diffractogram A indicated Cu, $Cu_2O$ and NaH crystals present. Diffractogram B indicated a mixture of $Cu_2O$ and Cu whilst that of C showed predominantly $Cu^0$. The XRD diffractogram showed that, surplus NaH was undissolved after step A before addition of methanol but it was consumed for the formation of the co-catalyst, $NaOCH_3$ upon addition of methanol, as illustrated in Eq. (7), hence the pressure rise of the mixture during the step B in Fig. 1.

The X-ray diffractogram for C (Fig. 2a) showed mainly $Cu^0$ reflections with an average crystallite size of 10 ± 1 nm. This indicates a slight increase in the average Cu particle size during the LTMS reaction. The metallic $Cu^0$ phase observed after methanol synthesis was not surprising considering the presence of a highly reducing environment made up of 20 bar of $H_2$ and CO mixture at 100 °C for 2 h. An XPS study of the chemical state of Cu catalyst has shown that 2 bar of syngas reduces $Cu^{2+}$ to $Cu^0$ at 250 °C in 1 h while at 100 °C, $Cu^{2+}$ reduces to $Cu^+$ [19]. Therefore, considering the presence of $Cu^+$ and $Cu^0$ after step B, further reduction of the remaining $Cu^+$ to $Cu^0$ at 100 °C observed in this work is in order.

The average crystallite size of $Cu_2O$ was estimated to be 7.6 ± 0.8 nm from XRD line broadening using the Rietveld analysis for B (Fig. 2b). The observed $Cu_2O$ rather than expected $Cu^0$ could be due to presence of some amount of oxygen in the reaction system. Glavee et al. [20] observed that borohydride reduction of $Cu^{2+}$ in water or diglyme yielded $Cu^0$ with stoichiometric release of $H_2$, when done under vacuum, however isolation of the Cu under ambient condition resulted in some amount of $Cu_2O$. Oxygen is also known to be soluble in organic solvents such as ethers with the solubility following the hydrocarbon chain length [21]. Therefore, the oxygen source could be dissolved oxygen in the solvent since the reaction was not done under vacuum.

Fig. 3a and b show the TEM images of the Cu catalyst after steps A and B respectively. Since the sample preparation for TEM imaging involved addition of MeOH to all samples, both A and B were expected to give similar Cu particles sizes. The particle sizes were around 10 ± 5 nm with some agglomerates. The observed particle sizes fall within the range of the crystallite size estimated for B from the XRD which was around 7.6 ± 0.8 nm.

Fig. 3c shows TEM imaging and the electron diffraction after the LTMS reaction. Here the particles were about 10 ± 3 nm. The image appeared to give a narrower particle size distribution as compared to that of the initial steps A and B. Again, the average crystallite size estimated by XRD was similar to the observed particle sizes by TEM. Electron diffraction showed the particles to be polycrystalline and indexing confirmed a metallic Cu phase to be present.

### 3.2. Deactivation test of the catalyst system

Multiple charging of the catalyst system was performed to investigate the recycle stability of the Cu catalyst system. The test sequence was similar to the first sequence (Fig. 1) except that the catalyst concentration was slightly higher. Syngas was charged to about 20 bar, heated to 100 °C and stirred to react for 2 h after which the reactor was cooled to about 25 °C and then degassed. This was repeated for 6 times as shown in Fig. 4a. Fig. 4b shows syngas conversion and selectivity for 7 consecutive charges. Syngas conversion decreased after each consecutive batch from 92% (1st charge) to 61% (6th charge). Selectivity to methanol and methyl formate were 94 and 6% respectively after the sixth charge. Liquid sampling for analysis was done just before and after the sixth charge so as not to reduce the amount of catalyst.

Syngas conversion decreased by 31% from the first to sixth charge. Since there are two components of catalysts involved, approximately 31% addition of one of the component should restore activity if that is responsible for the deactivation. As a consequence of that, 8 mmol NaH in 49 mmol MeOH was injected into the reactor. This represents a 31% increase of the initial methoxide content in the reactor. The syngas conversion increased slightly to 70% with 95 and 5% selectivity to methanol and methyl formate respectively. This indicated that even with 31% increase in the amount of co-catalyst, conversion increased by 9% with no significant change in selectivity. The 99.8% anhydrous MeOH purity used in the methoxide co-catalyst contain some ppm of water (≤0.002% according to the product specification sheet). However the total contribution of this to the conversion if methoxide reacted with water should by < 0.02% which is insignificant in our conversion range. This suggested that methoxide may not be the main or the only source of deactivation.

The Cu catalyst was characterized by XRD and TEM after the sixth charge which is shown in Fig. 5. A sharper and more intense Cu diffraction peak was observed for the sample of the 6th charged (spent catalyst) as compared to the fresh sample (i.e. sample slurry before the 1st charge), which showed predominantly $Cu_2O$ phase. The crystallite size was 16 ± 1 nm for the spent catalyst sample while that of the fresh sample was 8 ± 1 nm. The TEM image of the spent catalyst after the 6th charge showed a wide particle size distribution ranging from 6 to about 25 nm though the larger sizes dominated. Estimation of surface area ratio between the fresh Cu catalyst and spent catalyst after the 6th charge based on the Cu crystallite sizes from the XRD and Eq. (5) is 2.

Figs. 4b and 5 can be compared to Figs. 2a and 3c to make some inferences. First of all, the oxidation state of Cu after the 1st and 6th charge was $Cu^0$. Despite the fact that $Cu_2O$ was the starting component, the high activity of the Cu catalyst already after the first charge suggests that the probable active Cu phase of the Cu for LTMS reaction is $Cu^0$. An earlier, in-situ XPS study has shown Cu to be reduced during syngas conversion to MeOH at 100 °C [19]. Since our reaction conditions exposes the Cu catalyst system to 20 bar syngas which is expected to be a highly reducing atmosphere for Cu, metallic Cu surface is suspected to be active in the LTMS reaction.

Secondly, Cu crystallite and particle size after the 6th charge had increased significantly. Clearly there is an approximate doubling of crystal size between the 1st and the 6th charge. An estimation based on

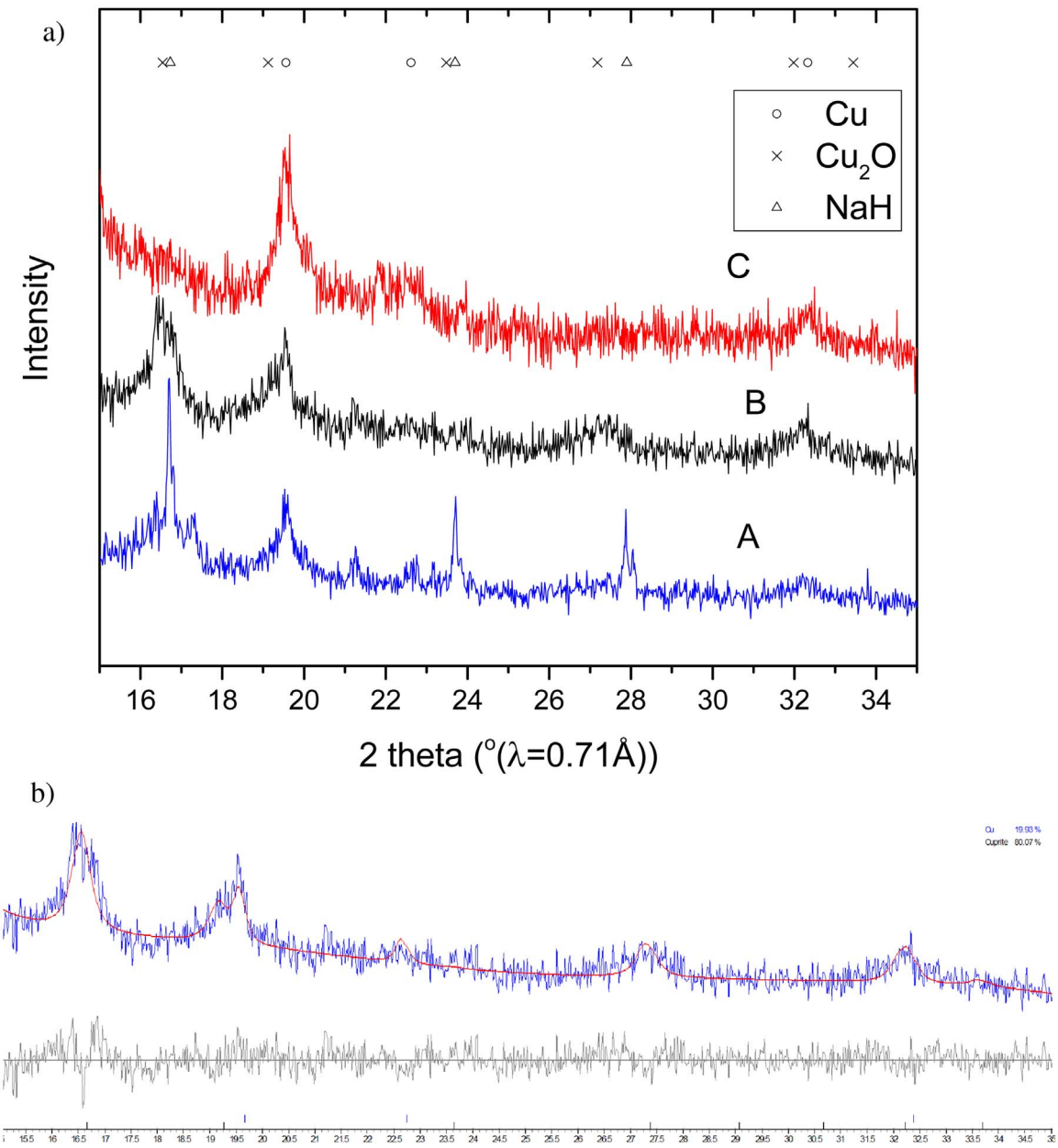


**Fig. 2.** X-ray diffractogram of the slurry at the different stages in Fig. 1. a: X-ray diffractogram of the slurry after the steps A, B and C. b: Rietveld analysis of diffffractogram B in Fig. 2.

Eq. (5) for the effect of agglomeration gives a surface area ratio between the 1st and 6th charge to be 1.6. This is comparable to the decline in syngas conversion of about 1.5 (=92/61). That is, there is a strong correlation between the reduction of active Cu surface available and the catalyst deactivation. On the other hand, it has also been suggested elsewhere [9] that the slight catalyst deactivation in LTMS reaction is due to the high sensitivity of alkoxide to $CO_2$ and $H_2O$ which may be formed in trace amounts during methanol synthesis as a byproduct. Although there is a possibility of some ppm of water in the anhydrous MeOH used as the source of the methoxide, this will not be adequate to cause the repetitive decline of catalytic activity. This notwithstanding, our observations point towards gradual decline of activity not only due to the alkoxide deactivation but rather due to a contribution from less available active site of the Cu nanoparticles.

The observed decline of activity after the successive batches can be attributed to loss of available active Cu surface. Although the reactants, CO and $H_2$ can compete for available Cu active sites, the degassing of the gas after successive batches ensures less effect from CO poisoning from previous batches. Moreover, our observed reduction of surface area after the successive batches suggests that the number of Cu active sites for the reactions reduced. Considering that the methyl formate hydrogenolysis is an exothermic reaction [22], increase in temperature of the reaction at the Cu surface during hydrogenation occurs, which can lead to the agglomeration of the Cu nanoparticles with time. Cu crystallite sintering is known to be a common deactivating factor to Cu catalysts [23]. Cu surface energy is expected to be high with around 10 nm Cu particles without any support, such that reacting with each other to form bigger crystals is highly possible[24]. We suggest therefore that the starting 'Cu' catalyst is soft or porous but agglomerates over time which led to decrease in the number of Cu active site for MeOH synthesis.

### 3.3. Varying Cu catalyst particle sizes with temperature

The Cu catalyst preparation was varied to study the influence of temperature on crystallite size and subsequently on LTMS reactivity. Fig. 6a shows the X-ray diffractogram of the effect of temperature on Cu catalyst preparation (same as steps A and B in Fig. 1). Preparation

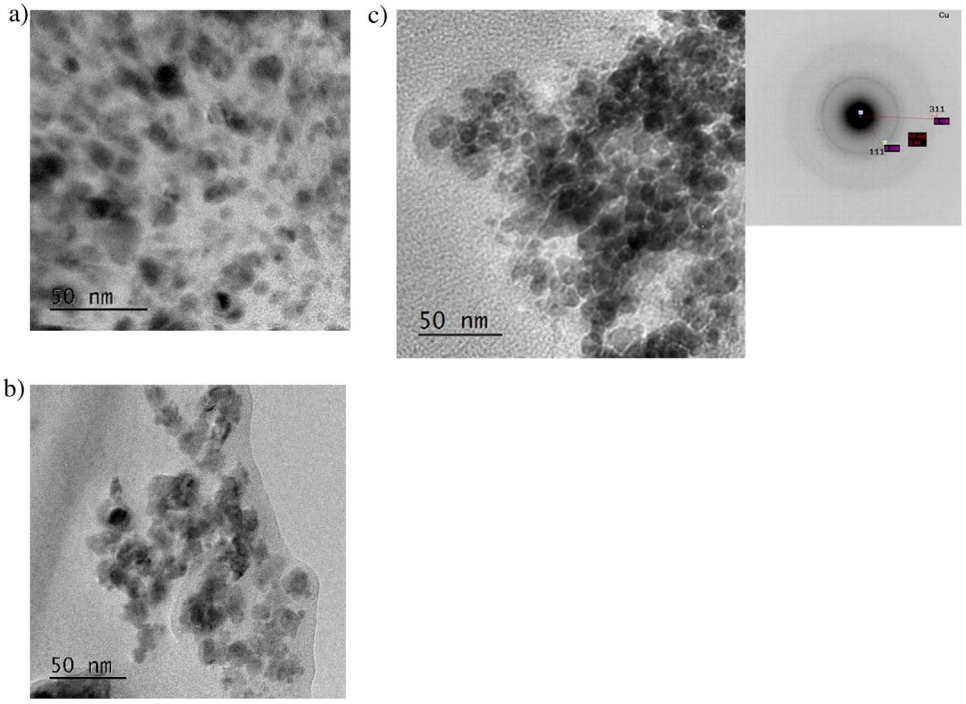


**Fig. 3.** Catalyst slurry TEM images of Cu nanoparticles for a typical 100 °C LTMS reaction shown in Fig. 1. a: TEM image after step A showing 10 ± 5 nm particle sizes. b: TEM image after step B showing 10 ± 5 nm particle sizes. c: TEM image after step C showing 10 ± 3 nm particle sizes.

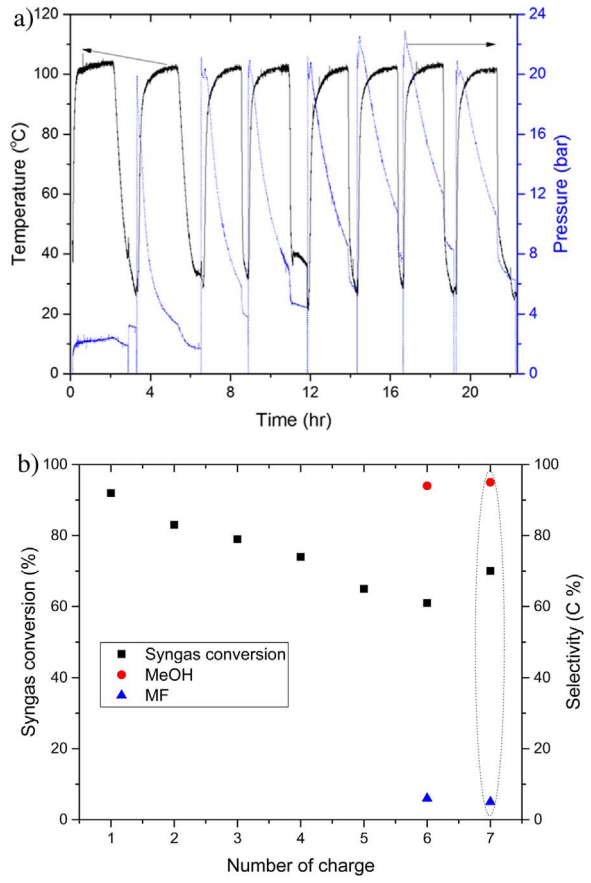


**Fig. 4.** Multiple charging of syngas, $Cu(OAc)_2$ = 5.0 mmol, NaH = 25 mmol, in 50 ml diglyme, MeOH = 73.0 mmol and $2H_2$:CO = 20 bar, at 100 °C. a: Temperature and pressure procedure of the multiple charging, cooling and degassing of syngas showing repeated charging over time. b: Syngas conversion and selectivity of the multiple charging of syngas reaction.

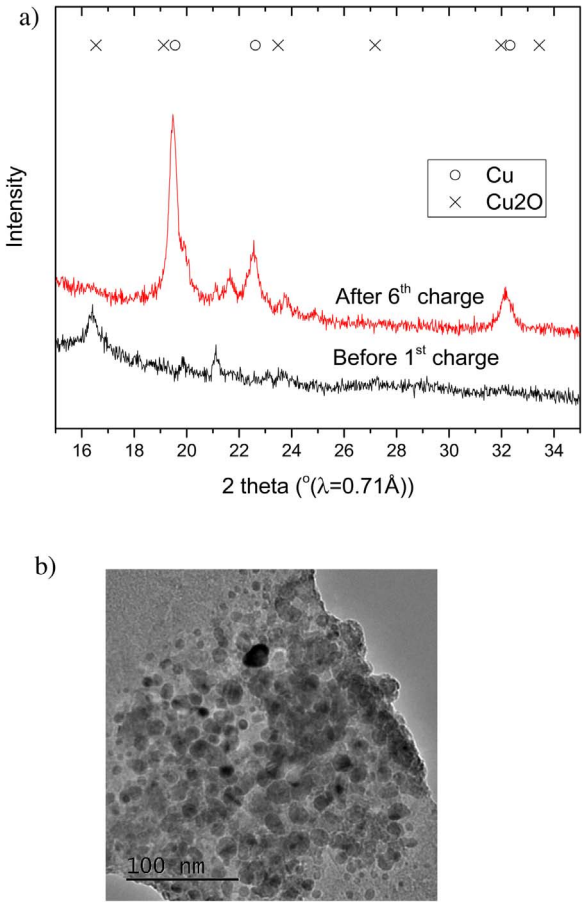


**Fig. 5.** X-ray diffraction and TEM image of spent Cu catalyst slurry (+ XRD of fresh). a: X-ray diffractogram of fresh (before 1st charge) and spent (after 6th charge) slurry of the LTMS reaction. b: TEM image after the 6th charge showing wide particle size distribution from 6 to 25 nm.

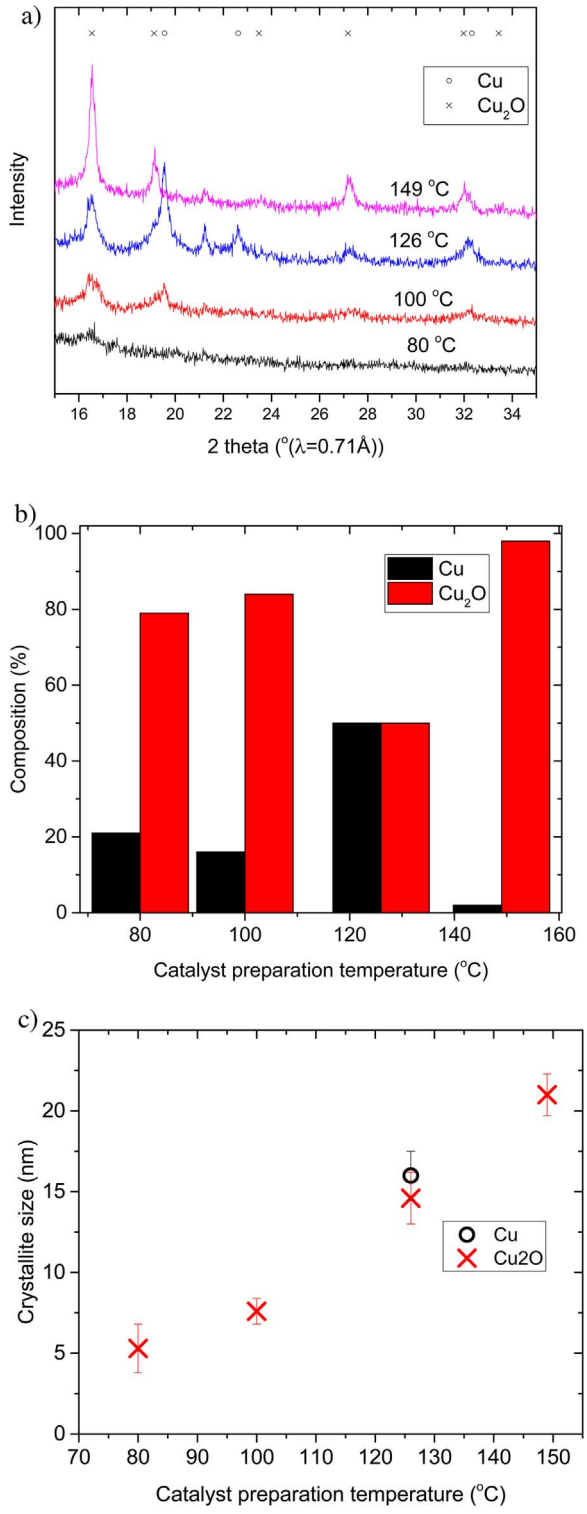


**Fig. 6.** X-ray diffractogram analysis of Cu crystallites before LTMS reaction. a: X-ray diffractogram of the slurry of the catalyst system. b: Rietveld analysis of the composition of Cu crystallites. c: Rietveld analysis of Cu crystallite sizes before LTMS reaction.

temperature was varied from 80 to 149 °C. Generally, the diffraction pattern showed that the intensity and sharpness of the peaks followed an increase in the temperature. The X ray shows densification of the Cu as temperature increased. This suggested that crystallization is enhanced by temperature.

The results of a Rietveld analysis of the diffraction patterns is shown in Fig. 6b and c for% composition of the Cu phases and their respective crystallite sizes. Increased fraction of $Cu_2O$ and less of $Cu^0$ was

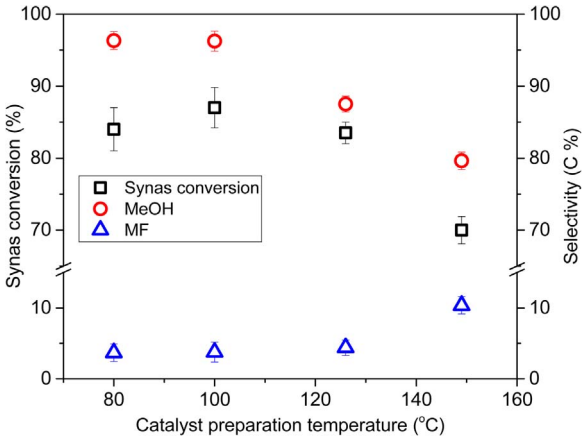


**Fig. 7.** Syngas conversion and selectivity verses catalyst preparation temperature; Cu $(OAc)_2$ = 3.6 mmol, NaH = 18 mmol in 50 ml diglyme, MeOH = 49 mmol, $2H_2$:1CO = 20 bar, at 100 °C.

observed, similar to the 100 °C catalyst system, except at 126 °C, which showed a composition of about 50/50 $Cu_2O/Cu^0$. This result indicated that reduction of the Cu takes place during catalyst preparation just as was discussed for catalyst preparation at 100 °C. The crystallite sizes were observed to exponentially increase with temperature, with the average size increasing from 5 ± 2 nm at 80 °C to 21 ± 1 nm at 149 °C. This is in agreement with theory [25] since particle nucleation exponentially depends on temperature.

The different nanoparticles were tested in the LTMS reaction at 100 °C similar to step C in Fig. 1. Fig. 7 shows conversion and selectivity versus catalyst system prepared at different temperatures. The syngas conversion was about 84, 89, 83, and 65% at 80, 100, 126, and 149 °C Cu catalyst systems respectively. Each test was done thrice and the average and standard deviations plotted. The selectivity to methanol was 96, 96, 88, and 80% at 80, 100, 126, and 149 °C catalyst systems respectively.

Syngas conversion and selectivity to MeOH were highest for the 80 and 100 °C catalyst systems. The Cu particles prepared under these temperatures resulted in producing Cu crystallites below 10 nm which the smallest compared to those which were prepared at higher temperatures. The syngas conversion for the 80 °C catalyst system was slightly lower than that of the 100 °C system. This could be due to less amount of Cu actually crystalizing out of solution at 80 °C within the reaction time considering the fact that temperature enhanced crystal growth, coupled with the observed very low intensity of the diffraction peaks in Fig. 6a. Though the 126 °C system produced about 83% syngas conversion, the 88% selectivity to MeOH was lower compared to that of 80 and 100 °C systems. Hence, the yield of MeOH generally decreased with increasing Cu crystallite size.

The reaction slurry was characterized by XRD and TEM at the end of the LTMS reaction. Fig. 8a shows the XRD diagrams of the spent slurry after the LTMS. The diffraction pattern shows predominantly the $Cu^0$ phase. Fig. 8b shows the results of the Rietveld analysis of the diffraction patterns shown in Fig. 8a as compared to the fresh crystallite sizes before the LTMS reaction. Generally, the average Cu crystallite sizes increased by about 2 nm for each catalyst system after the methanol synthesis.

The spent Cu catalyst was also studied by TEM imaging in order to compare Cu particle size distributions at the different preparation temperatures. Fig. 9 the TEM images of the Cu catalyst system prepared at varied temperatures. The Cu particle sizes were about 7 ± 4 nm for the 80 °C system. At 126 °C preparation, Cu particles sizes were about 18 ± 6 with some agglomerates up to 40 nm. The particles sizes were about 25 ± 6 and up to 50 nm agglomerates for the 149 °C system. The particles prepared at 100 °C were shown earlier to be about 10 ± 5 nm (Fig. 3c). Generally, the catalyst system prepared at 100 °C showed a

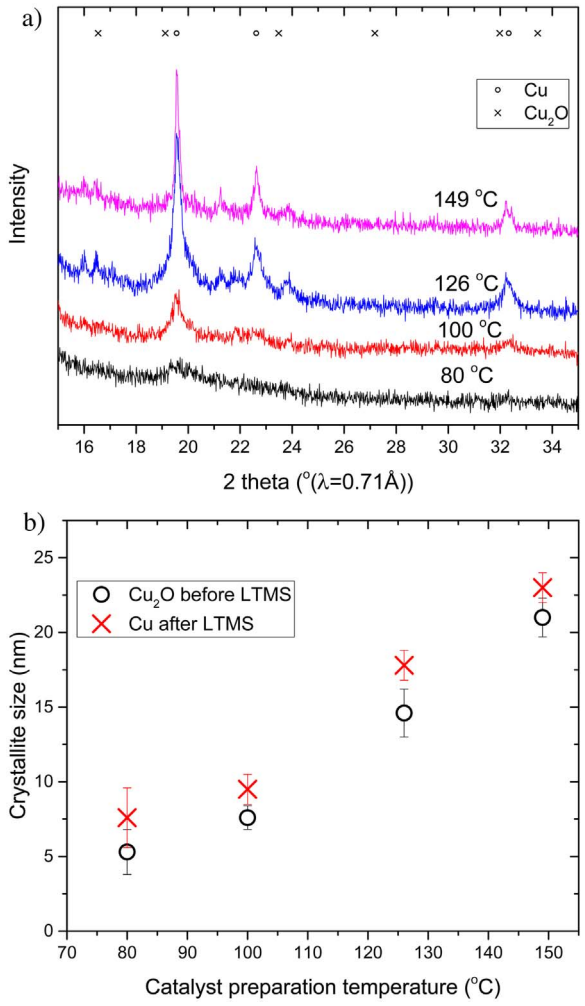


**Fig. 8.** X-ray diffractogram analysis of Cu crystallites after LTMS reaction. a: X-aray diffractogram of the slurry of the catalyst system. b: Rietveld analysis of Cu crystallite sizes.

much narrower particle distribution than the other systems. This could be due to the fact that both catalyst preparation and the LTMS reaction were done at the same temperature and therefore maintained a stable particle size as smaller particles often fuse together.

All in all, the particle sizes increased exponentially from about 3–50 nm agglomerates with increasing catalyst preparation temperature. This follows a similar pattern as was observed from the X-ray diffraction crystallite size estimations. In general, there are reports of strong correlation between particle size and the surface area [14,26]. Ohyama and Kishida [14] for example, reported an increase in surface area of $CuO/CrO_3$ due to milling, which enhanced activity of methanol production. The smaller the particle size, the more the available surface area is exposed per gram catalyst. Therefore if Cu is an active component, then methanol production increased with decreasing particle size. In our case, using traditional methods [27] to estimate Cu surface area would be challenging and not representative of the actual surface area as higher temperature than we operated is required. Nevertheless, the decrease in activity correlated well with densification of Cu nanoparticles.

## 4. Conclusion

We have used a once-through system for methanol synthesis at 100 °C. Hydride reduction of $Cu^{2+}$ in diglyme at varied temperatures led to $Cu^0$ nanocrystals varying from 5 to 23 nm in size. Increasing temperature from 80 to 149 °C increased the crystallite sizes of the

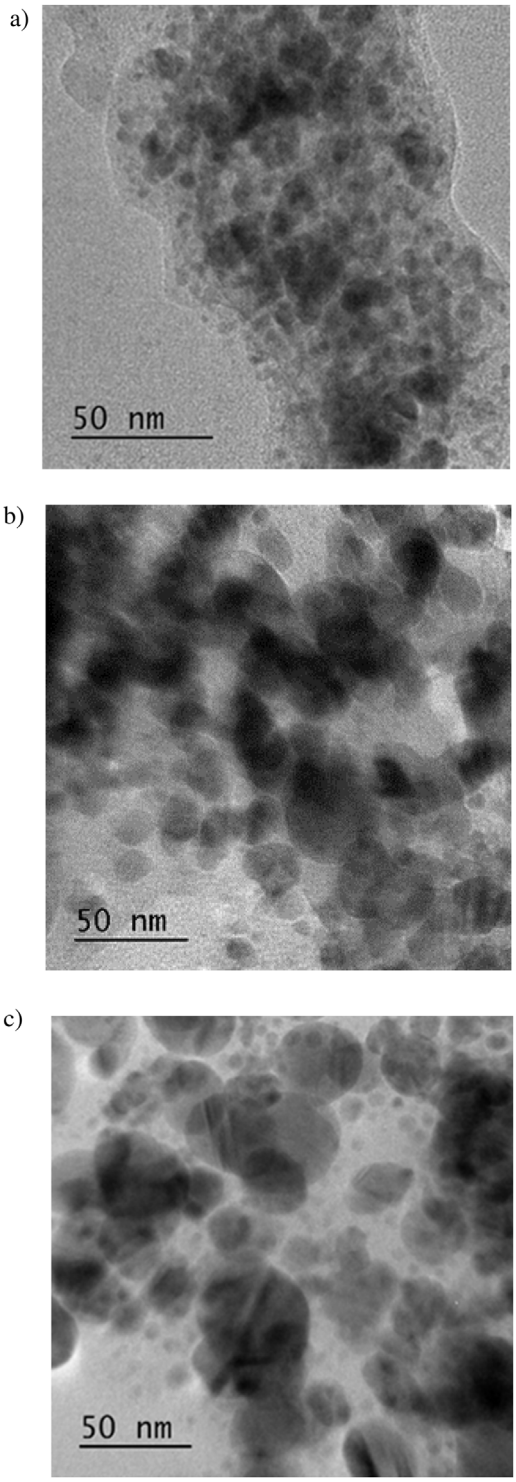


**Fig. 9.** Catalyst slurry TEM image of Cu catalyst prepared at varied temperatures after LTMS reaction. a: Catalyst system prepared at 80 °C showing 7 ± 4 nm particle sizes. b: Catalyst system prepared at 126 °C showing 18 ± 6 nm particle sizes. c: Catalyst system prepared at 149 °C showing 25 ± 6 nm particle sizes.

nanoparticles exponentially. Up to 92% conversion and 94% selectivity to methanol could be achieved at 100 °C and 20 bar syngas in liquid medium depending on Cu catalyst size. Generally, increasing particle size led to lower MeOH yield, and hence the smaller the nanoparticles the higher the methyl formate hydrogenolysis activity. The Cu nanoparticles densify over time during the catalytic process, which is proposed to be the major catalyst deactivation route.

## Acknowledgements

This work is funded by the Research Council of Norway, NFR project number 228157/O70.

We acknowledge the use of RECX (the Norwegian national resource center for X-ray diffraction and scattering) and NorTEM (the Norwegian Center for Transmission Electron Microscopy) both in Oslo.

## References

[1] G.A. Olah, Beyond oil and gas: the methanol economy, Angew. Chem. Int. Ed. 44 (2005) 2636–2639.
[2] U. Olsbye, S. Svelle, M. Bjørgen, P. Beato, T.V.W. Janssens, F. Joensen, S. Bordiga, K.P. Lillerud, Conversion of methanol to hydrocarbons: how zeolite cavity and pore size controls product selectivity, Angew. Chem. Int. Ed. 51 (2012) 5810–5831.
[3] K.A. Ali, A.Z. Abdullah, A.R. Mohamed, Recent development in catalytic technologies for methanol synthesis from renewable sources: a critical review, Renew. Sustain. Energy Rev. 44 (2015) 508–518.
[4] J.B. Hansen, P.E. Højlund Nielsen, Methanol synthesis, in: G. Ertl, H. Knozinger, F. Schuth, J. Weitkamp (Eds.), Handbook of Heterogeneous Catalysis, Wiley-VCH Verlag GmbH & Co KGaA, 2008, pp. 2920–2949.
[5] M. Marchionna, M. Di Girolamo, L. Tagliabue, M.J. Spangler, T.H. Fleisch, A review of low temperature methanol synthesis, in: D.S.F.F.A.V.A. Parmaliana, F. Arena (Eds.), Studies in Surface Science and Catalysis, Elsevier, 1998, pp. 539–544.
[6] J.A. Christiansen, Method of producing methyl alcohol, U.S. Patent 1,302,011, 1919.
[7] S.P. Tonner, D.L. Trimm, M.S. Wainwright, N.W. Cant, The base-catalysed carbonylation of higher alcohols, J. Mol. Catal. 18 (1983) 215–222.
[8] T. Turek, D.L. Trimm, N.W. Cant, The catalytic hydrogenolysis of esters to alcohols, Catal. Rev. 36 (1994) 645–683.
[9] S. Ohyama, Low-temperature methanol synthesis in catalytic systems composed of nickel compounds and alkali alkoxides in liquid phases, Appl. Catal. A: Gen. 180 (1999) 217–225.
[10] S. Ohyama, In situ FTIR study on reaction pathways in Ni(CO)4/CH3OK catalytic system for low-temperature methanol synthesis in a liquid medium, Appl. Catal. A: Gen. 220 (2001) 235–242.
[11] C. Voegtlin, Toxicity of Certain Heavy Metal Carbonyls, in: U.S.A.E. Commission (Ed.), University of Rochester, 1947.
[12] Z. Liu, J.W. Tierney, Y.T. Shah, I. Wender, Kinetics of two-step methanol synthesis in the slurry phase, Fuel Process. Technol. 18 (1988) 185–199.
[13] B. Li, K. Jens, Liquid-phase low-temperature and low-pressure methanol synthesis catalyzed by a raney copper-alkoxide system, Top. Catal. 56 (2013) 725–729.
[14] S. Ohyama, H. Kishida, Physical mixture of CuO and Cr2O3 as an active catalyst component for low-temperature methanol synthesis via methyl formate, Appl. Catal. A: Gen. 172 (1998) 241–247.
[15] S. Ohyama, H. Kishida, XRD, HRTEM and XAFS studies on structural transformation by milling in a mixture of CuO and Cr2O3 as an active catalyst component for low-temperature methanol synthesis, Appl. Catal. A: Gen. 184 (1999) 239–248.
[16] B. Li, K.-J. Jens, Low-temperature and low-pressure methanol synthesis in the liquid phase catalyzed by copper alkoxide systems, Ind. Eng. Chem. Res. 53 (2013) 1735–1740.
[17] https://www.bruker.com/products/x-ray-diffraction-and-elemental-analysis/x-ray-diffraction/xrd-software/topas/rietveld-analysis-software.html. (Date accessed: 28.10.2016).
[18] N.P. Fitzsimons, W. Jones, P.J. Herley, Studies of copper hydride. Part 1.-Synthesis and solid-state stability, J. Chem. Soc. Faraday Trans. 91 (1995) 713–718.
[19] T.H. Fleisch, R.L. Mieville, Studies on the chemical state of Cu during methanol synthesis, J. Catal. 90 (1984) 165–172.
[20] G.N. Glavee, K.J. Klabunde, C.M. Sorensen, G.C. Hadjipanayis, Borohydride reduction of nickel and copper ions in aqueous and nonaqueous media. controllable chemistry leading to nanoscale metal and metal boride particles, Langmuir 10 (1994) 4726–4730.
[21] R. Battino, T.R. Rettich, T. Tominaga, The solubility of oxygen and ozone in liquids, J. Phys. Chem. Ref. Data 12 (1983) 163–178.
[22] J.A. Christiansen, LIV.-The equilibrium between methyl formate and methyl alcohol, and some related equilibria, J. Chem. Soc. (Resumed) 129 (1926) 413–421.
[23] J.T. Sun, I.S. Metcalfe, M. Sahibzada, Deactivation of Cu/ZnO/Al2O3 methanol synthesis catalyst by sintering, Ind. Eng. Chem. Res. 38 (1999) 3868–3872.
[24] K.K. Nanda, A. Maisels, F.E. Kruis, H. Fissan, S. Stappert, Higher surface energy of free nanoparticles, Phys. Rev. Lett. 91 (2003) 106102.
[25] A.S. Myerson, R. Ginde, 2 − Crystals, Crystal Growth, and Nucleation, Handbook of Industrial Crystallization, Second edition, Butterworth-Heinemann, Woburn, 2002, pp. 33–65.
[26] K. Suttiponparnit, J. Jiang, M. Sahu, S. Suvachittanont, T. Charinpanitkul, P. Biswas, Role of surface area, primary particle size, and crystal phase on titanium dioxide nanoparticle dispersion properties, Nanoscale Res. Lett. 6 (2010) 1–8.
[27] J.R. Jensen, T. Johannessen, H. Livbjerg, An improved N2O-method for measuring Cu-dispersion, Appl. Catal. A: Gen. 266 (2004) 117–122.